Gold-Nanoparticle- and Gold-Nanoshell-Induced Polymorphism in Poly(vinylidene fluoride)

Wei Wang, Shishan Zhang, La-ongnuan Srisombat, T. Randall Lee,* Rigoberto C. Advincula*

PVDF nanocomposites are prepared through solution mixing of Au-NPs or Au-NSs with PVDF. The novel optical properties of Au-NPs and -NSs are retained as confirmed from UV-Vis spectra. Analysis of resulting nanocomposites by FT-IR, XRD, and DSC shows an obvious polymorphism change from α- to β-form compared to PVDF prepared under the same conditions. The β-polymorph seems to be more prominent with higher concentration of Au-NPs (0.5%) and even more so with Au-NSs. Thermogravimetric analysis shows that both nanocomposites have better resistance toward thermal degradation. Combination of novel optical properties of Au-NPs or Au-NSs with induced ferroelectric-active β-polymorph in PVDF can lead to new design of optical, piezoelectric devices.

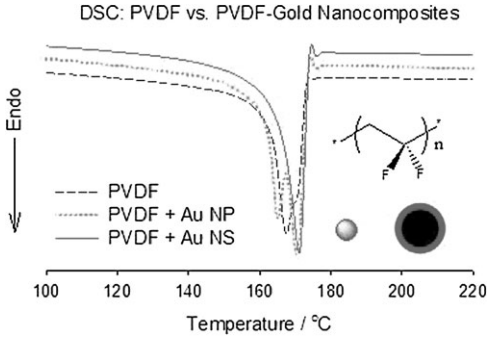

Introduction

Poly(vinylidene fluoride) (PVDF) is an important class of ferroelectric polymers.[1] When poled under high voltage, it exhibits efficient piezoelectricity and pyroelectricity, important properties widely utilized in transducer, actuator, and sensor applications.[2] The ferroelectricity of PVDF is closely associated with its crystalline structure. There are five different polymorphs for PVDF (α, β, γ, δ, and ε).[3] The most common polymorph of PVDF is the α-phase with a monoclinic unit cell and TGTG chain conformation.[4] Both β- and γ-polymorphs are orthorhombic, while the former possesses all-trans chain conformation[5] and the latter T3GT3G conformation.[6] The δ- and ε-polymorphs are polar and antipolar analogs of the α- and γ-forms, respectively.[7] Among all polymorphs of PVDF, only the β-phase is ferroelectrically active.

The combination of PVDF with nanomaterials to form polymer nanocomposites has recently been an interesting strategy to promote β-polymorph within the polymer phase and therefore enhance its ferroelectricity. Generally speaking, incorporation of nanoscale materials into a polymer matrix has a profound effect on the crystallization behavior and crystalline morphology, which might lead to an improvement of thermal and mechanical properties of polymers. For example, the addition of saponite into nylon 6 leads to the γ-phase, which improves the toughness of the polymer.[8] A combination of PVDF and nanoclay, as reported by Priya and Jog, transforms the crystalline structure from the usual α-polymorph to β-polymorph.[9] A similar polymorph change has also been observed with other PVDF nanocomposites prepared from single wall carbon nanotubes (SWNTs)[10] and silver nanoparticles.[11] The crystalline transformation of such procedures certainly favors the ferroelectricity of PVDF and leads to enhanced pyroelectric response and mechanical transduction.

W. Wang, S. Zhang, L. Srisombat, T. R. Lee, R. C. Advincula
Department of Chemistry and Department of Chemical and Biomolecular Engineering University of Houston, Houston, TX 77204, USA
Fax: +1 281 754 4445; E-mail: trlee@uh.edu
Fax: +1 713 743 1755; E-mail: radvincula@uh.edu

© 2011 WILEY-VCH Verlag GmbH & Co. KGaA, Weinheim

DOI: 10.1002/mame.201000271

Following this thread, we explored the possibility of dispersing gold nanomaterials, including nanoparticles and nanoshells, into PVDF for a gold/PVDF nanocomposite with a twofold purpose in mind. First, the addition of gold nanocrystals into PVDF might lead to the polymorph change favoring the ferroelectric properties of PVDF; secondly, the novel optical characteristic of gold nanomaterials can be integrated within the host polymer. The gold nanoparticles (Au-NPs) with size from tens of nanometers down to a few nanometers show an intense absorption band due to the collective electronic response of the metal to light, or otherwise known as plasmon resonance.[12] The wavelength of the plasmon band depends on particle size, shape, surface charge, and chemical environment surrounding it.[13] The gold nanoshells (Au-NSs) are a new type of optically tunable nanoparticles composed of a dielectric (most commonly, silica) core coated with an ultra-thin gold layer.[14] By changing the relative core and shell thickness, the absorbance of Au-NSs can be varied across a broad range of the optical spectrum that spans the visible and the near-IR spectral regions.

In this study, we demonstrate that PVDF nanocomposites containing Au-NPs or Au-NSs can be successfully prepared through solution mixing. The Au-NPs used here have an average diameter of 15 nm.[15] The Au-NSs are silica/gold core/shell composites with a silica core ≈100 nm covered with a gold shell of 25 nm thickness.[16] The PVDF nanocomposites are characterized by means of various spectroscopic techniques as well as thermal analysis. The novel optical properties of Au-NPs and Au-NSs are retained as confirmed by UV-Vis spectra. Analysis of the resulting nanocomposites by Fourier-transform infrared spectroscopy (FT-IR), X-ray diffraction (XRD), and differential scan calorimetry (DSC) shows an obvious polymorphism change from α- to β-form compared to PVDF prepared under the same conditions. The induced ferroelectric-active β-polymorph, along with the optical characteristics of gold nanomaterials dispersed in PVDF, could lead to development of technologically interesting optical, piezoelectric devices.

Experimental Part

Materials

PVDF [$\overline{M}_w \approx 180\,000$ according to gel permeation chromatography (GPC), $\overline{M}_n \approx 71\,000$] was acquired from Aldrich and used as received. The procedures described below were used to prepare 15 nm water-soluble Au-NPs and Au-NSs with ≈100 nm silica cores and ≈25 nm Au shell thicknesses.[15,16]

Preparation of Au-NPs[15]

In a 1 L round-bottom flask equipped with a condenser, 500 mL of 10^{-3} M $HAuCl_4$ was brought to boiling with vigorous stirring. Quick addition of 50 mL of 38.8×10^{-3} M sodium citrate to the vortex of the solution resulted in a color change from pale yellow to cherry red. The heating mantle was removed after 10 min, and stirring was continued for another 15 min. The resulting solution of Au-NPs was characterized by means of an absorption peak at 520 nm. Transmission electron microscopy (TEM) indicated a particle diameter of 15 ± 2 nm.

Preparation of Au-NSs[16]

The so-called Au-NSs are silica/gold core/shell composites with a silica core ≈100 nm covered with a shell of gold with a thickness of 25 nm. The gold shell was formed with the aid of seeding 2–3 nm gold colloidal clusters on the surface of the silica core. A detailed description of preparation is described below.

The silica core particles with a diameter of ≈100 nm were prepared by a slight modification of the well-known Stober method.[16a] 6.0 mL of ammonia (30% NH_3 as NH_4OH assay) was added to 100.0 mL of absolute ethanol. The mixture was stirred vigorously for 5 min before adding 3.0 mL (13.4 mmol) of tetraethylorthosilicate (TEOS). After 30 min, the solution changed from clear to opaque white. The concentration of the resultant silica nanoparticle was $\approx 7 \times 10^{12}$ particles $\cdot$ mL^{-1}. The silica nanoparticles were spherical in shape with ≈100 nm diameters as previously determined by means of scanning electron microscopy (SEM) and TEM.[16b] The surfaces of the silica nanoparticles were consequently functionalized with 3-(aminopropyl)trimethoxysilane (APTMS). An excess of APTMS (0.28 mmol) was added to a 100 mL aliquot of stirred silica nanoparticle solution and the mixture was allowed to react for 24 h. The solution then was refluxed at 80 °C for 1 h to enhance the covalent bonding of the APTMS groups to the silica nanoparticle surface. SEM and TEM results showed no big differences between the un-functionalized silica nanoparticles and functionalized silica nanoparticles.

Gold that had dimensions of 2–3 nm in diameter were routinely obtained using the procedure outlined.[16b] A 0.50 mL of 1 M NaOH and 1.0 mL of tetrakis(hydroxymethyl)phosphonium chloride (THPC) solution [prepared by adding 0.067 mmol of THPC to 1.0 mL of Milli-Q water] were added into a 45 mL aliquot of Milli-Q water. After stirring the reaction mixture for 5 min with a strong vortex in the reaction flask, 2.00 mL (27 mmol) of 1% $HAuCl_4$ in Milli-Q water was added quickly to the solution while stirring. Afterwards, the mixture was stirred for about 30 min and the color of the solution very quickly changed from colorless to dark reddish-brown. 10 mL of concentrated colloidal Au-NPs was mixed with 1 mL of APTMS-coated silica nanoparticles and was set aside to sit overnight to allow the colloidal Au-NPs to assemble on the surfaces of silica nanoparticles. The solution was then centrifuged and the resulting nanoparticles were redispersed in Milli-Q water. The color of the solution (Au/APTMS/silica nanoparticles) was light red after redispersing in Milli-Q water.

0.025 g of K_2CO_3 was dissolved in 100 mL of Milli-Q water in a reaction flask. After stirring for 10 min, 2.00 mL of 1% $HAuCl_4$ in water was added. The solution (K-gold solution) changed from yellow to colorless within 30 min. 0.50 mL of the Au/APTMS/silica nanoparticle solution was then added to a vigorously stirred 4 mL portion of prepared K-gold solution. After the reaction mixture was stirred for 10 min, 0.02 mL of formaldehyde was added to the reaction mixture. The solution changed from colorless to blue

© 2011 WILEY-VCH Verlag GmbH & Co. KGaA, Weinheim

within 2–4 min, which, for this procedure, is characteristic of nanoshell formation. The Au-NSs were then centrifuged and redispersed in Milli-Q water until use.

Preparation of the Nanocomposites

The gold (Au) nanomaterials were dispersed into PVDF by mixing 1% (w/v) PVDF solution in *N*,*N*-dimethylformamide (DMF) with 0.5×10^{-3} M (in terms of gold) Au-NPs or Au-NSs in H_2O. DMF was chosen due to its good solubility of PVDF and good miscibility with water in all proportions.[17,18] The mass ratio of gold over PVDF in mixture was varied from 0.5, 0.1 to 0.05%. The mixed solution was ultrasonically blended for 5 min and then dried on a Petri dish over a hot plate at 60 °C. The resulting polymer films were further dried and cured in vacuum at 60 °C for 36 h. A blank PVDF film was also obtained as reference at the same condition (including DMF/H_2O composition) for each polymer nanocomposite prepared.

Characterization

Spectroscopy

UV-Vis absorption spectra of both DMF solution and polymer films were obtained on an Agilent 8453 UV-Vis spectrophotometer. FT-IR spectra of dried polymer films were recorded using Digilab FTS 7000 Series spectrometer. Spectra (4 000–700 cm^{-1}) were collected from 256 scans at 4 cm^{-1} resolution with a mercury/cadmium telluride (MCT) detector. Nitrogen purged atmosphere was used as the background.

XRD

XRD studies were conducted for the dried and annealed polymer films using a Siemens D5000 X-ray diffractometer. The instrument was operated at a 40 kV voltage and 30 mA current, and scanned from $2\theta = 5$ to 42° at the step scan mode (step size 0.04°, preset time 2 s). The polymer films were glued onto a glass sample holder by using 3M Spra-Ment™ Craft & Display adhesive. A background diffractogram was also taken for comparison.

Thermal Analysis

Thermogravimetric analysis (TGA) was performed using a TGA 2050 Thermogravimetric Analyzer from TA Instruments. The sample was heated under nitrogen atmosphere (70 $cm^3 \cdot min^{-1}$) at a rate of 10 °C · min^{-1} from room temperature to 1 000 °C. DSC melting endotherms of polymers were obtained using DSC 2920 differential scanning calorimeter (TA Instruments) under nitrogen flow (50 $cm^3 \cdot min^{-1}$). The samples were heated at a rate of 5 °C · min^{-1} from ca. 40 up to 250 °C. Multiple heating scans were taken for each sample.

Results and Discussion

UV-Vis Characterization

The preparation of gold/PVDF nanocomposite requires the use of mixed solvents, DMF and H_2O, since the as-prepared gold nanomaterials are water-soluble only, while the polymer is best dissolved in polar organic solvent such as DMF or *N*,*N*-dimethylacetamide (DMAc). DMF was chosen due to its good solubility of PVDF and good miscibility with water in all proportions.[17,18] The process of mixing DMF solution of PVDF and the aqueous solution of Au-NPs/NSs was facilitated by sonication. There was no precipitation observed, and the resulting solution was clear by visual inspection.

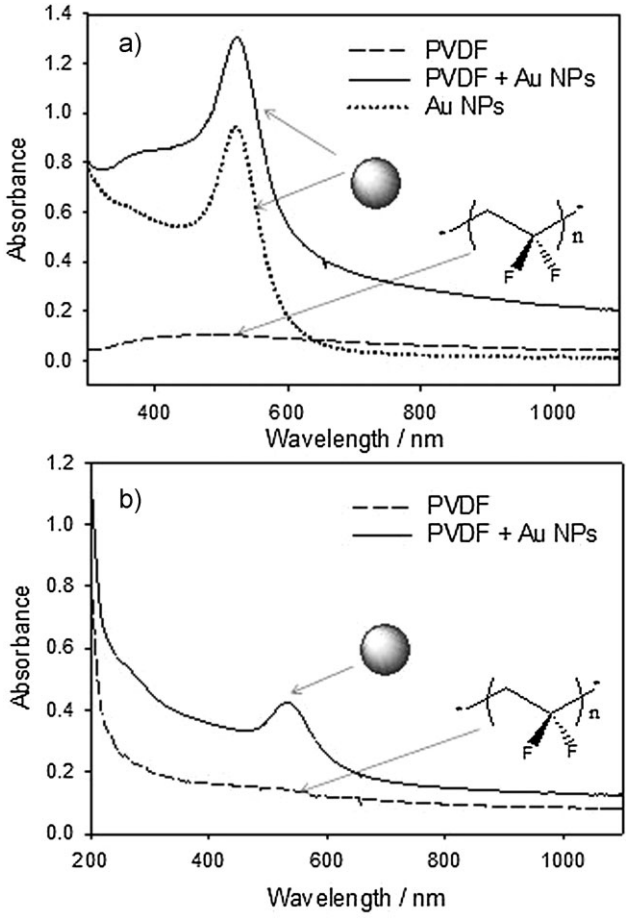

Figure 1. UV-Vis spectra from (a) 15 nm Au-NPs, PVDF, and gold/PVDF nanocomposites in mixed solvents of DMF and water, and (b) dried polymer films of either PVDF or gold/PVDF nanocomposite (as referenced to air), prepared from mixed solvents of DMF and water. The mass ratio of gold over PVDF in the mixture is 0.5%.

The UV-Vis spectra of Au-NPs, PVDF and mixture of both in solutions are presented in Figure 1(a), all of which are referenced to the blank, mixed solvents of DMF and H_2O. The 15 nm Au-NPs, prepared by sodium citrate reduction procedures, show an absorption band at a wavelength of ca. 520 nm, widely accepted as a result of surface plasmon (SP) resonance.[12] The UV-Vis of PVDF shows little absorption, due to the lack of chromophore, in the wavelength range scanned. The mixture of both is more or less a simple superposition of features from Au-NPs and

© 2011 WILEY-VCH Verlag GmbH & Co. KGaA, Weinheim

PVDF, alone. There is no shift of SP band observed with the added PVDF/DMF solution.

The shift of SP band is, however, detected by UV-Vis in the dried polymer/polymer composite films as shown in Figure 1(b). The solid-state UV-Vis measurement shows a SP band at 531 nm. The slight (10 nm) red shift of resonance is interesting and could have several origins: (i) first of all, aggregation or size change of nanoparticles during film preparation cannot be completely ruled out, despite the fact that isolated Au-NPs (≈15 nm) were observed under TEM. The red shift of the plasmon band can be due to increasing size of nanoparticles.[13] (ii) There is change of solvation state from solution to polymeric solid state. (iii) The refractive index of organic media surrounding Au-NP in PVDF is different from aqueous solution where SP band is normally observed. Underwood and Mulvaney have reported the effect of solvent refractive index on the SP band of Au-NPs.[19] A red shift of the resonance was observed to accompany the increase of refractive index of surrounding media, which was in excellent agreement with the predictions from Mie theory. In our case, the higher refractive index of PVDF (1.42) compared to water (1.33) may have caused the red shift. (iv) Strong dipole interaction between $-CF_2-$ of PVDF polymer chain and nanoparticles could be important as has been suggested in the study of other PVDF nanocomposites prepared from nanomaterials including silver nanoparticles, carbon nanotubes, and clay particles.[9–11] Existence of such interaction with Au-NPs are confirmed from IR, thermal analysis and XRD results shown below.

Besides Au-NPs, a polymer composite containing Au-NSs is also prepared using the same strategy as nanoparticles. UV-Vis spectra of solution samples and dried polymer films are illustrated in Figure 2, respectively. Similar to the case of Au-NPs, UV-Vis spectra of mixture of PVDF and Au-NSs, again, incorporate the features mainly from the nanoshells since there is little absorption for PVDF itself at a wavelength of 400 nm or longer. The 25 nm thickness Au-NSs, prepared on a 100 nm diameter spherical silica core, exhibit a broad absorption band starting from 580 nm and extending into the deep IR region.[16] The special optical characteristics of Au-NSs are intact when mixed with PVDF in dilute solution [Figure 2(a)] but seem less obvious in dried films due to the higher scattering background in solid-state films [Figure 2(b)]. Successful incorporation of IR absorbing nanomaterials into PVDF provides a potential opportunity to harness the thermal energy from solar irradiation and further convert such energy into electric power due to the pyroelectric nature of the polymer.[1]

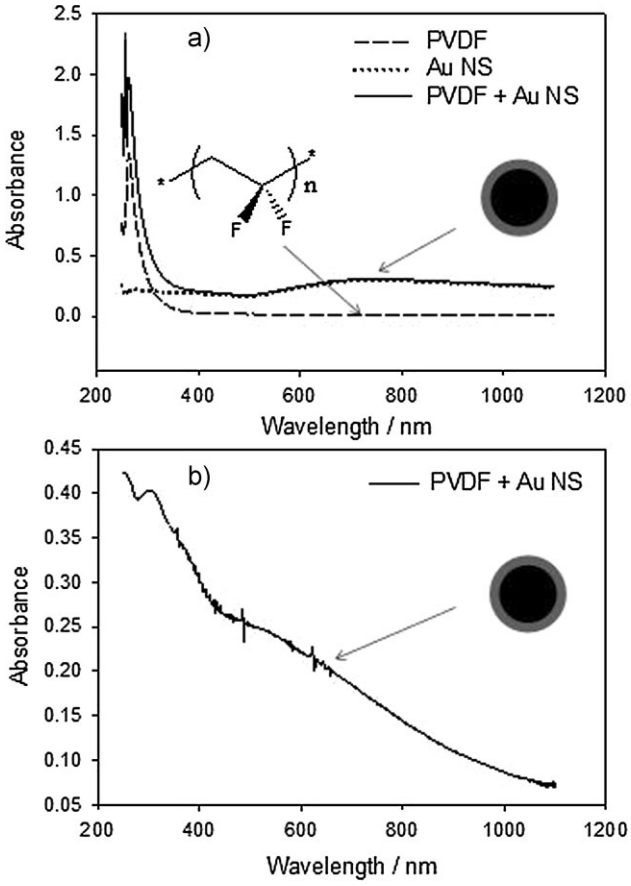

Figure 2. UV-Vis spectra from (a) 25 nm Au-NS on 100 nm silica core, PVDF and Au-NS/PVDF composite in mixed solvents of DMF and water, and (b) dried polymer film of Au-NS/PVDF composites (as referenced to pure PVDF), prepared from mixed solvents of DMF and water. The mass ratio of gold over PVDF in the mixture is 0.5%.

FT-IR Spectroscopy

The FT-IR spectra, taken from dried polymer films, are shown in Figure 3. Compared to PVDF itself, the most significant differences detected from the polymer films with dispersed 15 nm Au-NP are the peak features observed at 976 and 764 cm^{-1}. The 976 cm^{-1} peak is for the CH_2 twisting vibration while 764 cm^{-1} is responsible for the CF_2 bending and for the skeletal CF–CH–CF bending.[20] The absence of those two absorption peaks in the IR spectra from the polymer nanocomposite strongly suggests the possible electrostatic interaction between the CF dipoles in the polymer chain and the surface charge on Au-NP, a result resonating with the red-shift of SP band in UV-Vis as described above.[11]

Nandi and coworkers suggested, based on their measurements with silver polymer composite, that the interaction between PVDF and nanoparticles should straighten the PVDF backbone, leading to the formation of zigzag conformation (β-polymorph) instead of the coil TGTG conformation (α-polymorph).[11] The polymorph change should have been evident from IR spectra since, according to literature, α-polymorph depicts characteristic absorption at

© 2011 WILEY-VCH Verlag GmbH & Co. KGaA, Weinheim

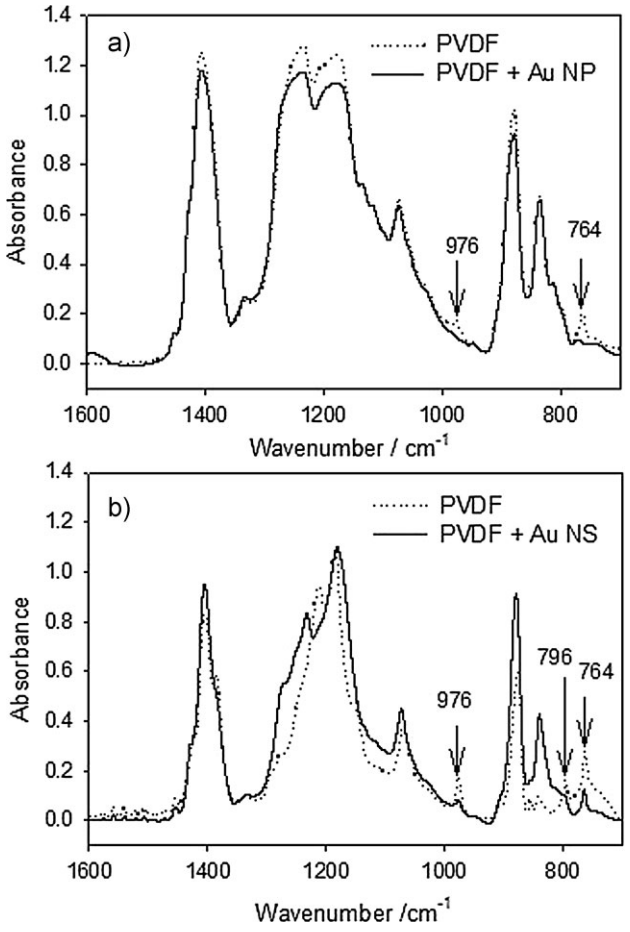

Figure 3. FT-IR spectra from dried polymer films of (a) PVDF and Au-NP/PVDF composite, and (b) PVDF and Au-NS/PVDF composite, prepared from mixed solvents of DMF and water. The mass ratio of gold over PVDF in the mixture is 0.5%.

796, 615, and 529 cm^{-1} while β-polymorph has peaks at 510 and 483 cm^{-1}.[21] Such features are not observed due to the lower limit (700 cm^{-1}) of our IR instrument. However, an observable change is indeed present at 796 cm^{-1} for the polymer films with dispersed Au-NSs, as illustrated in Figure 3. Besides the similar trend change at 976 and 764 cm^{-1} as seen with Au/NP polymer composite, the absence of absorption at 796 cm^{-1}, which is characteristic of α-polymorph, is evident for the polymer films after the inclusion of 25 nm thickness Au-NSs, which suggests a conversion of α-polymorph to other crystalline structures. This phenomenon was validated by thermal analysis.

Thermal Analysis

The polymorph change in PVDF due to the dispersion of Au-NPs/nanoshells can be also traced by thermal analysis. PVDF with β-polymorph has a higher melting point than that of α-form due to the better packing of the zigzag β-PVDF

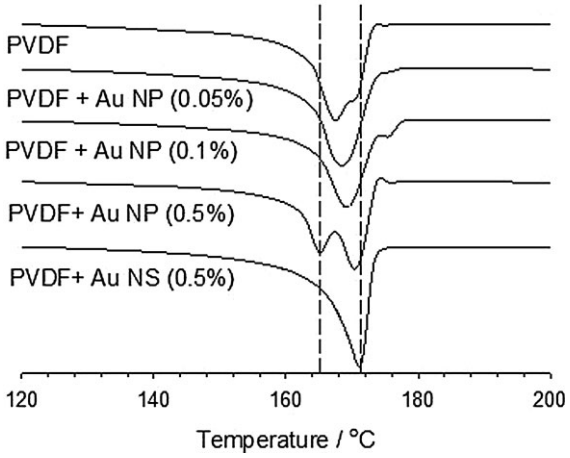

Figure 4. DSC melting endotherms of PVDF, Au-NP/PVDF composites with varied gold-to-PVDF mass ratios of 0.5, 0.1, and 0.01%, and Au-NS/PVDF composites with gold-to-PVDF mass ratio of 0.5%.

chain than that of the TGTG α-chain.[11] The inclusion of gold nanomaterials into PVDF should induce the change of thermal properties of its hosting polymer if the polymorph transformation from α to β takes place as we observed from the FT-IR spectra.

The DSC melting endotherms of PVDF and different nanocomposites are shown in Figure 4, and the melting temperatures are listed in Table 1. The observed melting temperatures for pure PVDF and nanocomposites with Au-NP content varied from 0.05, 0.1 to 0.5% are 167, 168, 169, and 171 °C, respectively. The higher melting temperature of PVDF nanocomposite supports our speculation of crystalline change in the polymer. The polymorph change might originate from the surface of Au-NP since there is a strong interaction between the polymer chain and nanoparticle surface as suggested from FT-IR measurements. The trend that higher content of Au-NP accompanies higher melting

Table 1. Melting temperature of PVDF and various Au/PVDF composites from DSC measurements.

Sample type	Au content	Melting temperature	
	wt.-%	°C	
		PVDF [a)]	PVDF + Au
Au-NP	0.05	167.3	168.2
	0.1	167.0	169.2
	0.5	167.3	170.9
Au-NS	0.5	167.3	170.9

[a)] A PVDF blank was prepared, under the same solution conditions, along with each nanocomposite.

© 2011 WILEY-VCH Verlag GmbH & Co. KGaA, Weinheim

temperature supports this speculation. The DSC result from Au-NS/PVDF composite is also included in Figure 4 and Table 1. A higher shift of melting temperature is obvious. The amount of shift is similar to that of Au-NP with same gold content (0.5%).

The polymorphism transformation from α- to β-form seems to trend with Au-NP content. While there are mixed polymorphs in PVDF reference as evidenced from the convoluted DSC melting peaks, the differences between the two polymorphs (α and β) are sharpening with increasing loading of Au. Two distinct melting peaks are observed with 0.5% of Au-NPs. Incorporation of Au-NS in PVDF shows predominantly the melting peak at higher temperature only, suggesting even higher β-polymorph content. The origin of this distribution is not readily explained at this point and might be related to size or the polarizability of the larger Au-NSs versus the smaller Au-NPs.

The decomposition of nanocomposites was also studied by means of TGA.[22] The resulting thermograms are illustrated in Figure 5. Apparently, pure PVDF exhibits a two-step decomposition process with 60–70% mass loss occurring at 478 °C for the first step and remaining mass loss finished at 1 000 °C (the upper limit of instrument).[22] The TGA thermogram of polymer composite containing Au-NPs is different in that, while the first step of degradation happens at a similar temperature with similar mass loss, the thermal degradation of the second step is much slower at temperature above 500 °C and undergoes possible multiple steps. The degradation of polymer composite is eventually incomplete at 1 000 °C with a remaining mass much higher than the total mass of Au-NPs added. Clearly, the decomposition of PVDF is not complete with the presence of Au-NPs. The resistance of nanocomposite toward thermal degradation may be related to the strong interaction between PVDF and Au-NPs and the latter nanoparticle stability. The strong interaction between nanoparticles and the host PVDF matrix is indicated by the UV-Vis and FT-IR spectra and further confirmed by the polymorph change (to more stable β-conformation) observed in DSC. Similar incomplete degradation behavior was also detected (Figure 5) on PVDF containing Au-NSs covering silica cores. Since there are no covalently-bonded ligands around the Au-NS,[16] the interaction with PVDF might directly involve the gold surfaces. As contrast, the surface of Au-NP prepared is normally stabilized with ionically bonded citrates.[15]

XRD

The direct evidence of polymorph change in the polymer can be obtained from the X-ray diffraction measurements. Shown in Figure 6 are the X-ray diffractograms of films prepared from PVDF and its nanocomposites. The pure PVDF exhibits peaks at $2\theta = 18.5$, 20.2, and 26.6°, characteristic of α-polymorph.[23] The significant change of diffrac-

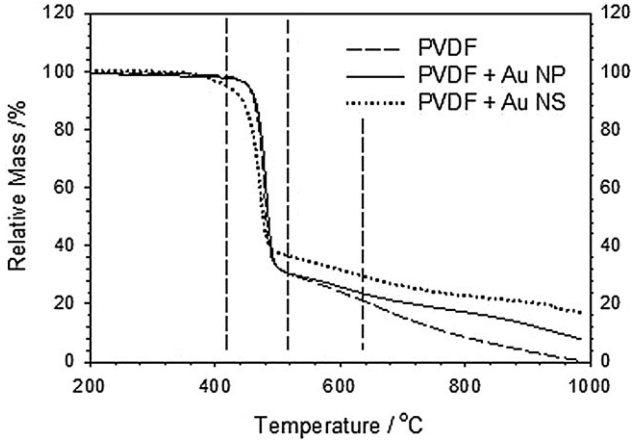

Figure 5. TGA thermograms of (a) PVDF and AU-NP/PVDF, and (b) PVDF and Au-NS/PVDF composites. The mass ratio of gold over PVDF in the mixture is 0.5%.

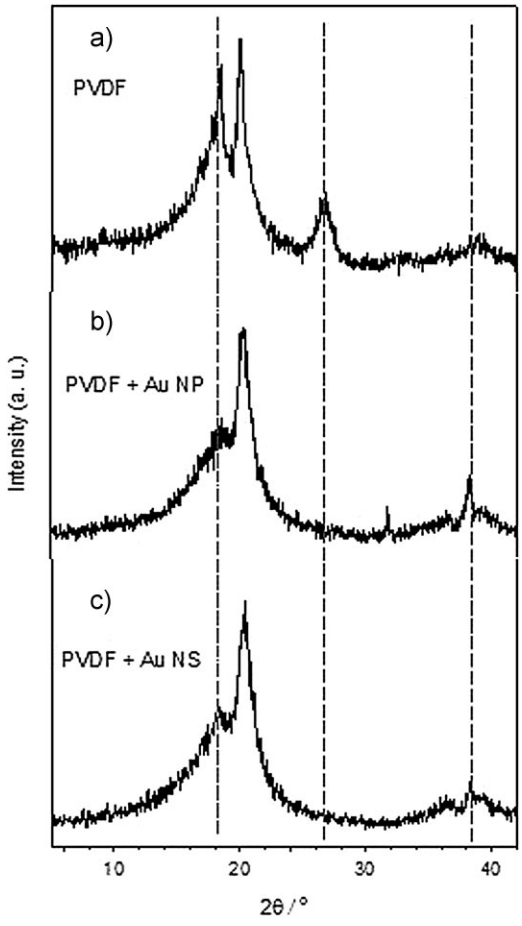

Figure 6. X-ray diffractograms of (a) PVDF, (b) Au-NP/PVDF, and (c) PVDF and Au-NS/PVDF composites. The mass ratio of gold over PVDF in the mixture is 0.5%.

© 2011 WILEY-VCH Verlag GmbH & Co. KGaA, Weinheim

tion pattern is observed after the inclusion of Au-NP/Au-NS in the polymer. The diffractogram of composite shows no peak at 18.5 and 26.6, but at 20.8°, which clearly characterizes a higher β-polymorph content.[24] A separate peak at ≈38° is also observed and ascribed to be from the crystal structure of Au-NPs [Au (111)].[25]

Conclusion

A series of PVDF nanocomposites were prepared by physical dispersion of 15 nm Au-NPs or 25 nm thick Au-NSs (on 100 nm silica core) in mixed DMF and water solution of PVDF. The resulting polymer composites, after drying and curing, were characterized by means of various spectroscopic methods. The novel optical properties of Au-NPs and -NS were largely retained as evident from UV-Vis spectra. XRD clearly demonstrates the polymorph change from α- to β-form as a result of inclusion of gold nanomaterials, which is also supported by FT-IR and DSC. The polymorph change is believed to be induced by the dipole interaction between PVDF and the Au-NPs dispersed. A thermodynamically stable zigzag conformation of PVDF chain is favored over TGTG chain orientation, resulting β-form dominated polymorph. The successful incorporation of gold nanomaterials into PVDF could lead to important applications in the areas of optical, piezoelectric sensor design and solar energy conversion. Retaining optical properties of Au-NPs or Au-NS in PVDF paves a path to the design of devices or sensors based on the optical characteristics of those gold nanomaterials. Furthermore, PVDF is a widely-used ferroelectric polymer that can effectively transform mechanical stress and/or temperature gradient to electrical potential. The piezoelectric properties of PVDF, when appropriately coupled with optical characteristics of gold nanomaterials, could prove to be a new way of solar energy conversion. The work concerning those two aspects is currently underway.

Acknowledgements: The authors would like to acknowledge generous funding from the *Robert A. Welch Foundation* (grant numbers E-1551 and E-1320).

Received: July 25, 2010; Revised: October 10, 2010; Published online: December 22, 2010; DOI: 10.1002/mame.201000271

Keywords: nanoparticles; nanoshells; piezoelectric; polymorphism; poly(vinylidene fluoride) (PVDF)

[1] [1a] T. Furukawa, *IEEE Trans. Elect. Insulation* **1989**, *24*, 375; [1b] A. I. Baise, H. Lee, B. Oh, R. E. Salomon, M. M. Labes, *Appl. Phys. Lett.* **1975**, *26*, 428; [1c] K. Koga, H. Ohigashi, *J. Appl. Phys.* **1986**, *59*, 2142; [1d] R. G. Kepler, R. A. Anderson, *J. Appl. Phys.* **1978**, *49*, 1232.
[2] [2a] H. Kawai, *Jpn. J. Appl. Phys.* **1969**, *8*, 975; [2b] G. M. Sessler, *J. Acoustical Soc. Am.* **1981**, *70*, 1596.
[3] A. J. Lovinger, in: *Developments in Crystalline Polymers 1*, D. C. Bassett, Ed., Applied Science Publishers, London 1981, p. 195
[4] [4a] W. W. Doll, J. B. Lando, *J. Macromol. Sci., Phys. B* **1970**, *4*, 309; [4b] R. Hasegawa, Y. Takahashi, Y. Chatani, H. Tadokaro, *Polym. J.* **1972**, *3*, 600.
[5] [5a] T. T. Wang, J. M. Herbert, A. M. Class, in: *The Applications of Ferroelectric Polymers*, Blackie & Sons Ltd., London 1988; [5b] J. B. Lando, H. G. Olf, A. Peterlin, *J. Polym. Sci.* **1966**, *4*, 941.
[6] S. Weinhold, M. Litt, J. B. Lando, *J. Polym. Sci.* **1979**, *17*, 585.
[7] A. K. Nandi, L. Mandelkern, *J. Polym. Sci., Part B: Polym. Phys.* **1991**, *29*, 1287.
[8] T. M. Wu, C. S. Liao, *Macromol. Chem. Phys.* **2000**, *201*, 2820.
[9] L. Priya, J. P. Jog, *J. Appl. Polym. Sci.* **2003**, *89*, 2036.
[10] N. Levi, R. Czerw, S. Xing, P. Iyer, D. L. Carroll, *Nano Lett.* **2004**, *4*, 1267.
[11] S. Manna, S. K. Batabyal, A. K. Nandi, *J. Phys. Chem. B* **2006**, *110*, 12318.
[12] M. J. Hostetler, J. E. Wingate, C.-Z. Zhong, J. E. Harris, R. W. Vachet, M. R. Clark, J. D. Londono, S. J. Green, J. J. Stokes, G. D. Wignall, G. L. Glish, M. D. Porter, N. D. Evans, R. W. Murray, *Langmuir* **1998**, *14*, 17.
[13] [13a] J. Turkevich, P. C. Stevenson, J. Hillier, *Discuss. Faraday Soc.* **1951**, *11*, 55; [13b] J. Turkevich, G. Garton, P. C. Stevenson, *J. Colloid Sci.* **1954**, *9*, 26; [13c] C. L. Haynes, R. P. Van Duyne, *J. Phys. Chem. B* **2001**, *105*, 5599.
[14] [14a] J.-H. Kim, W. W. Bryan, T. R. Lee, *Langmuir* **2008**, *24*, 11147; [14b] J.-H. Kim, W. W. Bryan, H.-W. Chung, C. Y. Park, A. J. Jacobson, T. R. Lee, *ACS Appl. Mater. Interfaces* **2009**, *1*, 1063.
[15] [15a] G. Frens, *Nat. Phys. Sci.* **1973**, *241*, 20; [15b] K. C. Grabar, R. G. Freeman, M. B. Hommer, M. J. Natan, *Anal. Chem.* **1995**, *67*, 735.
[16] [16a] W. Stöber, A. Fink, E. Bohn, *J. Colloid Interface Sci.* **1968**, *26*, 62; [16b] T. Pharm, J. B. Jackson, N. J. Halas, T. R. Lee, *Langmuir* **2002**, *18*, 4915.
[17] H. Bipp, H. Kieczka, in: *Ullmann's Encyclopedia of Industrial Chemistry*, 5th edition, Wiley-VCH Weinheim 1989, p. A12/1-12.
[18] A. Bottino, G. Camera-Roda, G. Capannelli, S. Munari, *J. Membr. Sci.* **1991**, *57*, 1.
[19] S. Underwood, P. Mulvaney, *Langmuir* **1994**, *10*, 3427.
[20] R. E. Belke, I. Cabasso, *Polymer* **1988**, *29*, 1831.
[21] [21a] S. Enomoto, Y. Kawai, M. Sugita, *J. Polym. Sci., Part A-2* **1968**, *6*, 861; [21b] K. Tashiro, M. Kobayashi, *Phase Transitions* **1989**, *18*, 213; [21c] G. Cortili, G. Zerbi, *Spectrochim. Acta, Part A* **1967**, *23*, 2216.
[22] [22a] S. Zulfiqar, M. Zulfiqar, M. Rizvi, A. Munir, I. C. McNeill, *Polym. Degrad. Stab.* **1994**, *43*, 423; [22b] L. F. Malmonge, L. H. C. Mattoso, *Polymer* **2000**, *41*, 8387.
[23] Y. Takahashi, H. Tadokoro, *Macromolecules* **1980**, *13*, 1317.
[24] [24a] J. B. Lando, W. W. Doll, *J. Macromol. Sci. Phys.* **1968**, *B2*, 205; [24b] G. Guerra, F. E. Karasz, W. J. MacKnight, *Macromolecules* **1986**, *19*, 1935.
[25] X. Feng, C. Mao, G. Yang, W. Hou, J. Zhu, *Langmuir* **2006**, *22*, 4384.

© 2011 WILEY-VCH Verlag GmbH & Co. KGaA, Weinheim